Midinfrared frequency comb from self-stable degenerate GaAs optical parametric oscillator

Kevin F. Lee,[1,*] C. Mohr,[1] J. Jiang,[1] Peter G. Schunemann,[2] K. L. Vodopyanov,[3] and M. E. Fermann[1]

[1]*IMRA America, Inc., 1044 Woodridge Avenue, Ann Arbor, Michigan 48105, USA*
[2]*BAE Systems, P.O. Box 868 Nashua, New Hampshire 03063, USA*
[3]*CREOL, College of Optics and Photonics, Univ. Cent. Florida, Orlando, FL 32816, USA*
[*]*klee@imra.com*

Abstract: We pump a degenerate frequency-divide-by-two optical parametric oscillator (OPO) based on orientation-patterned GaAs with a stable Tm frequency comb at 2 micrometer wavelength and measure the OPO comb offset frequency and linewidth. We show frequency division by two with sub-Hz relative linewidth of the comb teeth. The OPO thermally self-stabilizes and oscillates for nearly an hour without any active control.

OCIS codes: (190.4970) Parametric oscillators and amplifiers; (190.4975) Parametric processes; (140.6810) Thermal effects.

References and links

1. N. Leindecker, A. Marandi, R. L. Byer, and K. L. Vodopyanov, "Broadband degenerate OPO for mid-infrared frequency comb generation," Opt. Express **19**(7), 6296–6302 (2011).
2. A. Marandi, N. C. Leindecker, V. Pervak, R. L. Byer, and K. L. Vodopyanov, "Coherence properties of a broadband femtosecond mid-IR optical parametric oscillator operating at degeneracy," Opt. Express **20**(7), 7255–7262 (2012).
3. K. F. Lee, J. Jiang, C. Mohr, J. Bethge, M. E. Fermann, N. Leindecker, K. L. Vodopyanov, P. G. Schunemann, and I. Hartl, "Carrier envelope offset frequency of a doubly resonant, nondegenerate, mid-infrared GaAs optical parametric oscillator," Opt. Lett. **38**(8), 1191–1193 (2013).
4. A. S. Villar, K. N. Cassemiro, K. Dechoum, A. Z. Khoury, M. Martinelli, and P. Nussenzveig, "Entanglement in the above-threshold optical parametric oscillator," J. Opt. Soc. Am. B **24**(2), 249–256 (2007).
5. A. Marandi, N. C. Leindecker, K. L. Vodopyanov, and R. L. Byer, "All-optical quantum random bit generation from intrinsically binary phase of parametric oscillators," Opt. Express **20**(17), 19322–19330 (2012).
6. S. T. Wong, K. L. Vodopyanov, and R. L. Byer, "Self-phase-locked divide-by-2 optical parametric oscillator as a broadband frequency comb source," J. Opt. Soc. Am. B **27**(5), 876–882 (2010).
7. A. Foltynowicz, P. Masłowski, T. Ban, F. Adler, K. C. Cossel, T. C. Briles, and J. Ye, "Optical frequency comb spectroscopy," Faraday Discuss. **150**, 23–31 (2011).
8. S. T. Cundiff and J. Ye, "Femtosecond optical frequency combs," Rev. Mod. Phys. **75**(1), 325–342 (2003).
9. C.-C. Lee, S. Suzuki, W. Xie, and T. R. Schibli, "Broadband graphene electro-optic modulators with sub-wavelength thickness," Opt. Express **20**(5), 5264–5269 (2012).
10. N. Leindecker, A. Marandi, R. L. Byer, K. L. Vodopyanov, J. Jiang, I. Hartl, M. Fermann, and P. G. Schunemann, "Octave-spanning ultrafast OPO with 2.6-6.1 μm instantaneous bandwidth pumped by femtosecond Tm-fiber laser," Opt. Express **20**(7), 7046–7053 (2012).
11. V. O. Smolski, S. Vasilyev, P. G. Schunemann, S. B. Mirov, and K. L. Vodopyanov, "Cr:ZnS laser-pumped subharmonic GaAs optical parametric oscillator with the spectrum spanning 3.6-5.6 μm," Opt. Lett. **40**(12), 2906–2908 (2015).
12. J. Kiessling, Fraunhofer Institute of Physical Measurement Techniques, Heidenhofstraße 8, D-79110 Freiburg, Germany (personal comunication 2013).
13. T. Skauli, P. S. Kuo, K. L. Vodopyanov, T. J. Pinguet, O. Levi, L. A. Eyres, J. S. Harris, M. M. Fejer, B. Gerard, L. Becouarn, and E. Lallier, "Improved dispersion relations for GaAs and applications to nonlinear optics," J. Appl. Phys. **94**(10), 6447 (2003).
14. D. K. Serkland, R. C. Eckardt, and R. L. Byer, "Continuous-wave total-internal-reflection optical parametric oscillator pumped at 1064 nm," Opt. Lett. **19**(14), 1046–1048 (1994).
15. P. L. Hansen and P. Buchhave, "Thermal self-frequency locking of a doubly resonant optical parametric oscillator," Opt. Lett. **22**(14), 1074–1076 (1997).
16. A. Douillet, J.-J. Zondy, A. Yelisseyev, S. Lobanov, and L. Isaenko, "Stability and frequency tuning of thermally loaded continuous-wave $AgGaS_2$ optical parametric oscillators," J. Opt. Soc. Am. B **16**(9), 1481–1498 (1999).

#246889 Received 30 Jul 2015; revised 9 Sep 2015; accepted 11 Sep 2015; published 1 Oct 2015

17. P. Dubé, L.-S. Ma, J. Ye, P. Jungner, and J. L. Hall, "Thermally induced self-locking of an optical cavity by overtone absorption in acetylene gas," J. Opt. Soc. Am. B **13**(9), 2041–2054 (1996).
18. K. F. Lee, N. Granzow, M. A. Schmidt, W. Chang, L. Wang, Q. Coulombier, J. Troles, N. Leindecker, K. L. Vodopyanov, P. G. Schunemann, M. E. Fermann, P. St. J. Russell, and I. Hartl, "Midinfrared frequency combs from coherent supercontinuum in chalcogenide and optical parametric oscillation," Opt. Lett. **39**(7), 2056–2059 (2014).
19. K. F. Lee, P. Maslowski, A. Mills, C. Mohr, J. Jiang, C. C. Lee, T. R. Schibli, P. G. Schunemann, and M. Fermann, "Broadband Midinfrared Comb-Resolved Fourier Transform Spectroscopy," in CLEO: 2014, OSA Technical Digest (online) (Optical Society of America, 2014), paper STh1N.1.

1. Introduction

Degenerate optical parametric oscillators (OPOs) are noteworthy sources of broadband midinfrared frequency combs [1–3], entangled photons [4], and random number generation [5]. Their main advantages are a low oscillation threshold, typically 10 mW, broad bandwidth [1], and relatively good stability against vibrations [6]. They are often overlooked due to the interferometric stability requirement, but as a source of frequency combs, we find that a degenerate OPO can produce narrow comb lines at well-defined frequencies for hours without active stabilization, aided by self-stabilizing thermal feedback.

Degenerate OPOs were previously shown to produce output that is coherent with the pump laser by observing spatial and temporal interferences between the OPO output with a reference beam [5, 6]. Here, we make a quantitative measurement of the relative linewidth between the OPO and the pump comb to determine how well the OPO preserves the frequency comb nature of the pump. We find that the carrier envelope offset of the pump is cleanly divided by 2, and the relative linewidth is well below 1 Hz, meaning that the absolute frequency accuracy will usually not be limited by the OPO, but by the pump comb or its reference. This source may find use as a simple midinfrared comb source for new applications such as trace gas detection, or high-resolution spectroscopy [7].

2. Experiment

A frequency comb, being a regular set of spectral lines, can be defined by the comb spacing, which is the same as the laser repetition rate; and the shift of the comb relative to zero frequency, which is the carrier envelope offset (CEO) frequency, named for its relation to the carrier envelope offset phase of the laser pulse train [8]. In this experiment, outlined in Fig. 1, we pump our degenerate OPO with a stabilized frequency comb, and measure the resulting midinfrared frequency comb from the OPO.

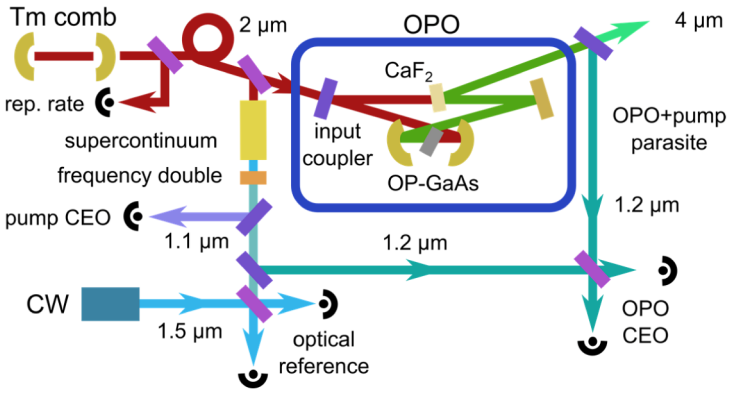

Fig. 1. System outline. A Tm frequency comb pumps a degenerate OPO, and supercontinuum generation in nonlinear fiber for comb stabilization. Interference between the upconverted OPO and supercontinuum is used to measure the frequency stability of the OPO comb.

Our OPO is synchronously pumped, meaning that the resonant midinfrared pulse is met by the next pump pulse when it arrives at the nonlinear crystal. This requires that the repetition

#246889 Received 30 Jul 2015; revised 9 Sep 2015; accepted 11 Sep 2015; published 1 Oct 2015

rate of the OPO is the same as the pump laser, leaving the OPO CEO to be measured. The OPO pump is a thulium fiber frequency comb with 100 fs pulse duration, 418 MHz repetition rate, and 2.5 W of average power. The wavelength ranges from 1.9 to 2.0 µm with the main peak from about 1940 to 1970 nm. About 1.8 W is used to pump the OPO, with the rest used to generate supercontinuum in highly nonlinear fiber that extends the pump comb from about 1.1 to 2.3 µm for carrier envelope offset (CEO) frequency stabilization by *f*-to-2*f* interferometry [8] using fast loss modulation from a graphene layer on a laser end mirror [9], and phase locking to a 1.5 µm wavelength optical reference with a specified short term linewidth of 3 kHz. Slow drift of the optical reference was stabilized by temperature feedback against the repetition rate, as measured against a GPS-disciplined Rb clock, with repetition rate drifts of less than 1 Hz on the second timescale.

The ring-cavity OPO uses a thin (0.5 mm along beam direction) orientation-patterned GaAs (OP-GaAs) crystal with a 53 µm reversal period placed at Brewster angle, similar to [10]. GaAs is among the most suitable materials for midinfrared generation, having high second order nonlinearity and transmission well beyond 10 µm. When degenerate, our OPO has a broad spectrum from about 3.3 to 5 µm, with exact bandwidth depending on cavity length and CEO, with examples in Fig. 2. The OPO input coupler transmits 2 µm light, while reflecting 3 to 6 µm light. A 1° wedge of CaF_2, about 1 mm thick, acts as both the dispersion compensator and the output coupler. Each output beam from the two wedge surfaces has about 40 mW average power. The OPO is purged to reduce humidity and carbon dioxide absorption.

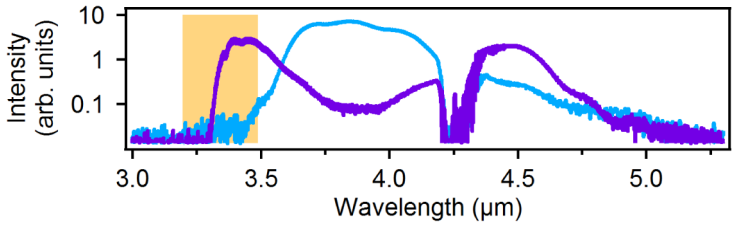

Fig. 2. Example spectra of the degenerate OPO with a pump CEO of 274 MHz (purple, broader spectrum), and 140 MHz (blue, narrower spectrum). The shaded area indicates wavelengths that can contribute to the beat with the pump supercontinuum. The broad absorption at 4.25 µm is from CO_2 in air.

In addition to the midinfrared output, the OPO crystal also generates parasitic combinations of OPO and pump frequencies. Sum frequency generation (SFG) of the pump and the OPO at 1.2-1.3 µm is relatively intense. Parasitic SFG at 1230 ± 10 nm is separated from the main output and spatiotemporally combined with the pump supercontinuum, and measured on balanced fast photodiodes to generate a radio frequency (RF) beat note providing a measure of the OPO CEO frequency. We can see this by writing the beat frequency as the difference of the SFG comb and the pump comb: $\nu_{beat} = (nf_{rep} + f_{OPO} + f_{pump}) - (mf_{rep} + f_{pump}) = (n\text{-}m)f_{rep} + f_{OPO}$, where f_{rep} is the repetition rate, f_{OPO} and f_{pump} are the carrier envelope offset frequencies, and n and m are integers. In the RF spectrum between 0 and f_{rep}, the OPO CEO will appear as a beat at f_{OPO} and $f_{rep} - f_{OPO}$.

For understanding the degenerate OPO comb frequencies [6], there are three main constraints: (i) signal and idler are the same (degenerate); (ii) photon energy conservation; and (iii) the repetition rate, and thus comb spacing, is the same as the pump (synchronously pumped OPO). Constraints (i) and (ii) imply that the OPO frequencies are the pump frequencies divided by two. Dividing all the pump comb lines would result in halving the OPO comb spacing as well, so either even $(2nf_{rep} + f_{pump})$ or odd $((2n + 1)f_{rep} + f_{pump})$ pump comb lines are divided at one time to maintain condition (iii). The result is two possible sets of OPO combs, with frequencies of $nf_{rep} + f_{pump}/2$ (even), or $nf_{rep} + f_{pump}/2 + f_{rep}/2$ (odd).

#246889 Received 30 Jul 2015; revised 9 Sep 2015; accepted 11 Sep 2015; published 1 Oct 2015

Adding $f_{rep}/2$ to the OPO CEO is like flipping the electric field, which is achieved in practice by moving to adjacent cavity-length resonances, toggling between the even and odd sets [5].

3. Frequency measurements

Degenerate OPO CEO coherence was previously observed through spatial and temporal interferences with the pump, a continuous wave intermediate [6], and a second degenerate OPO [2]. These measurements agreed with the expected OPO CEO values to MHz accuracy [6], and found the relative linewidth of the OPO comb was likely better than 20 kHz [2].

We set our pump CEO to different values, and measured the pump CEO, OPO CEO, and repetition rate by frequency counter to within ± 0.3 Hz or less, also referenced to a GPS-disciplined Rb clock. The repetition rate was stabilized to 417 690 000.0 Hz. Measured values are listed in Table 1. The ambiguity of identifying the positive and negative frequency beat replicas in the RF spectra can be resolved for the pump CEO by observing directions of change of the repetition rate relative to changes in the chosen *f*-to-2*f* beat while the pump comb is locked to the optical reference. We did not have a corresponding test for the OPO beat, and list the value in the table that corresponds to half of the pump CEO. Informal testing for other pump CEO frequencies also resulted in OPO CEO frequencies of half of the pump CEO frequency. From these measurements, we see that the degenerate OPO does exactly halve the pump frequency, as expected, to within 10^{-9} over long timescales.

Table 1. CEO frequencies of pump and degenerate OPO

Pump CEO (Hz)	OPO CEO (Hz)	Ratio
140 000 000.00	70 000 000.0	2.000 000 00
274 000 000.00	137 000 000.0	2.000 000 00
275 690 000.00	137 845 000.0	2.000 000 00
281 690 000.00	140 845 000.0	2.000 000 00

Being a doubly-resonant OPO, there are a few discrete resonant roundtrip cavity lengths, separated by the pump wavelength, at which the OPO will oscillate [1]. The OPO was degenerate for most of the longest OPO cavity length resonance. The short-cavity end of this resonance and all other resonances were nondegenerate. We label operation as degenerate based on the measured CEO rather than the spectrum, which does not clearly differentiate between the two.

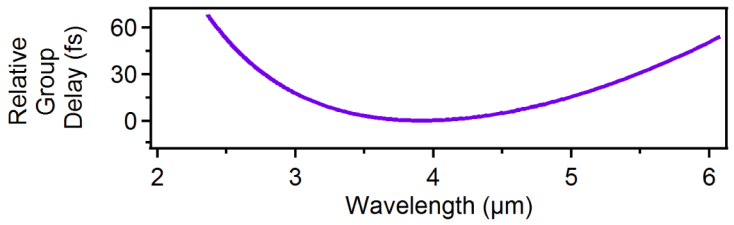

Fig. 3. Calculated group delay after passage through 0.5 mm of bulk GaAs, and 0.8 mm of CaF_2, referenced to the minimum delay. If the second-order dispersion is balanced for degeneracy near 4 μm, degenerate OPO pulses will be faster than nondegenerate pulses, corresponding to a longer cavity resonance. Nondegenerate pulses are slower, corresponding to a shorter cavity resonance.

The relation of cavity length to degeneracy comes from the group delay minimum at degeneracy resulting from dispersion balancing between the OP-GaAs crystal and the CaF_2 wedge, as illustrated in Fig. 3. A longer cavity better matches the lowest group delay at degeneracy, while a shorter cavity better matches the higher group delay of nondegenerate pulses with correspondingly shorter and longer wavelengths for the signal and idler waves.

To quantify the relative linewidth of the OPO, we used a fast Fourier transform analyser to take a high resolution RF spectrum of the OPO beat, shown in Fig. 4. Above 10 Hz, the pump

#246889 Received 30 Jul 2015; revised 9 Sep 2015; accepted 11 Sep 2015; published 1 Oct 2015

and OPO have very similar noise profiles. Below 10 Hz, the OPO shows more noise than the pump comb at the same timescale as the slow intensity and spectral fluctuations of the unstabilized OPO. While broader than the pump, the linewidth is still well below 1 Hz.

The odd comb line case is expected when the OPO roundtrip cavity length is increased by 2 μm, half of the OPO wavelength, corresponding to the electric field sign flip of the addition of $f_{rep}/2$ to the OPO CEO frequency [6]. In our OPO, this second resonance only operated nondegenerately, with distinct and cavity-length dependent signal and idler CEO frequencies [3]. The nondegenerate operation had beats near the expected $f_{pump}/2 + f_{rep}/2$ frequency, similar to the even comb line case where the beats from the nondegenerate modes are close in frequency to the degenerate value and move further away as the signal and idler separate in wavelength.

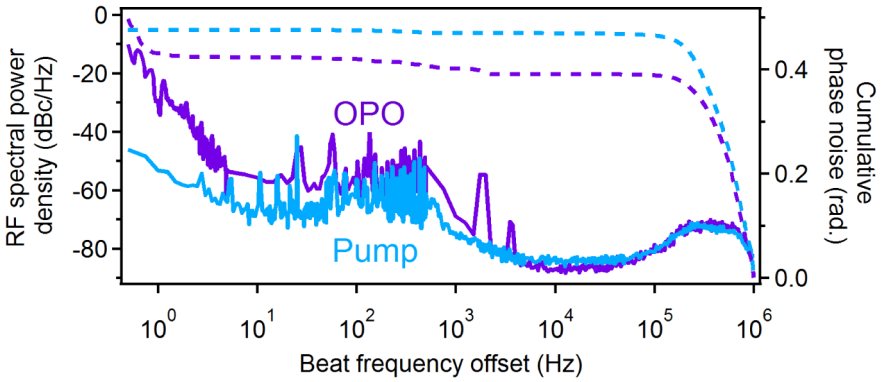

Fig. 4. Plot of the pump CEO, and OPO CEO RF beats (solid curves), and their associated cumulative phase noises (dashed). The OPO and pump have similar behaviour at high frequencies. The OPO has additional noise at low frequencies, but still maintains sub-Hz relative linewidth without any stabilization.

4. Output stability

With the pump comb stabilized, our OPO can passively maintain oscillation for nearly an hour as shown in Fig. 5. A photodiode verified continuous oscillation for 54 minutes. A frequency counter monitoring the OPO CEO beat confirms that the OPO had the degenerate CEO value of 94 MHz (half the pump CEO of 188 MHz), except for times around 15 minutes when it drifted into nondegeneracy. The low frequencies measured after 40 minutes are artifacts from a weaker beat frequency due to reduced OPO spectrum, the OPO was still degenerate as seen on an RF spectrum analyser.

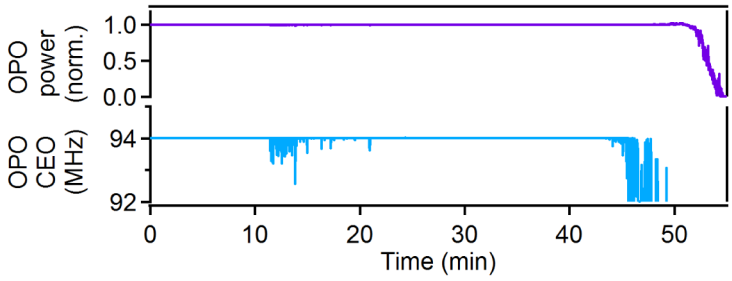

Fig. 5. Monitored OPO output and CEO beat. The pump CEO was 188 MHz. The OPO passively oscillates for 54 minutes, and stays degenerate except for the 15 minute region. The low CEO at the end is an artifact of reduced beat note intensity.

The long term stability is limited by our room temperature, which varies by 0.1 K over minutes, and drifts by about 1 K over hours. The intensity was very stable over the few

#246889 Received 30 Jul 2015; revised 9 Sep 2015; accepted 11 Sep 2015; published 1 Oct 2015

minute timescale, as shown in Fig. 6, which has a standard deviation of 0.38% when sampled at 1 kHz. When operating nondegenerately, the OPO can also oscillate passively, but any vibrations are directly mapped onto frequency shifts of the signal and idler CEO. While degenerate, vibrations and drifts will cause intensity and spectral bandwidth variations, but not significant frequency changes, resulting in a passively stable midinfrared frequency comb.

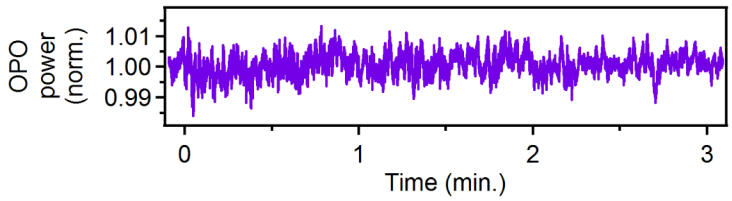

Fig. 6. Power stability of passive degenerate OPO over 3 minutes, measured at 1 kHz. The standard deviation is 0.38%.

To give a better sense of the difference in the frequency stability between degenerate and nondegenerate modes, Fig. 7 shows a low resolution beat note spectrum of the OPO and pump interference from an RF spectrum analyser with a sweep time of 0.5 s, and a resolution bandwidth of 10 kHz for degenerate (upper) and nondegenerate (lower) operation. Both RF spectra are referenced to a background measurement taken when the OPO is not oscillating. For this measurement, the pump CEO was locked to 70 MHz, but the pump oscillator length was not stabilized to test high-vibration conditions. While the degenerate case has a single narrow beat frequency at half of the pump CEO frequency, the nondegenerate beat note ranges over several MHz even though the cavity vibrations are the same in both cases.

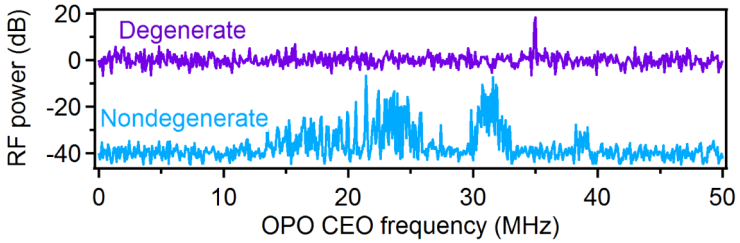

Fig. 7. RF spectrum of the OPO CEO frequency taken over 0.5 s for degeneracy (upper, purple) and nondegeneracy (lower, blue, offset by 40 dB) from the OPO parasite SFG and pump comb beat note. In the presence of the same noise sources, the degenerate case produces a single, narrow beat note, while the nondegenerate beat note moves over a large range of frequencies.

5. OPO thermal response

Besides the OPO reported here, another degenerate OPO was reported to be stable [6], but we have not observed such high stability in all of our OPOs. The distinguishing feature of our stable OPO is the high 418 MHz pulse repetition rate and the accompanying high 1.8 W pump power. Thermal effects from the strong pumping are clearly visible when tuning the cavity length in the two directions as shown in Fig. 8. Starting from a long cavity and shortening towards resonance results in a broad and asymmetric cavity resonance as seen on the left side of Fig. 8, while lengthening the cavity results in a much narrower resonance.

Given the seconds timescale of the cavity length hysteresis, we hypothesized that the hysteresis and self-stabilization are thermal effects. When we approach the OPO resonance from a longer cavity, the intracavity OPO power (centred at 4 μm) increases to about 2 W, as estimated from the output power. Even higher intracavity enhancement of four times the pump power has been reported in a different GaAs OPO with a low roundtrip loss of 10-20% and high 92% pump depletion [11]. Though small, the absorption of 4 μm radiation in GaAs

#246889 Received 30 Jul 2015; revised 9 Sep 2015; accepted 11 Sep 2015; published 1 Oct 2015

is enough to cause a local rise in the crystal temperature. In fact, OP-GaAs absorption at 3-4 μm was measured to be 3-10 times larger than at 2 μm [12]. Through positive dn/dT of 2×10^4 K^{-1} (crystal refractive index change with temperature) [13], the roundtrip cavity length effectively increases by about 0.1 μm/K. On the left side of Fig. 8, the degenerate OPO output increases with slowly shortening cavity length. The increased intensity results in heating that counteracts the mechanical shortening. Heating allows oscillation over about 0.8 μm of additional mechanical length change relative to the lengthening case (right side of Fig. 8), corresponding to about 8 K difference in crystal temperature. Similar effects have been observed in other OPOs [14–16] and passive cavities that contain absorbing gas [17].

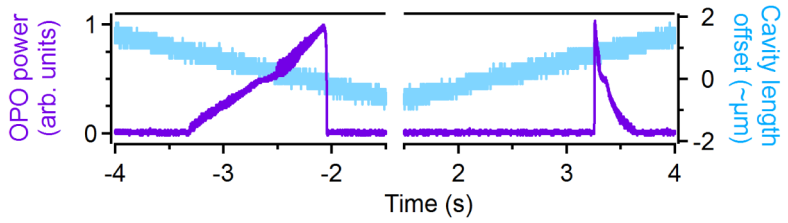

Fig. 8. OPO output (thin purple line) as roundtrip cavity length (thick blue line) is slowly shortened (left) then lengthened (right) through the mostly degenerate resonance (nondegenerate at the highest output). The different peak widths are due to crystal heating which counteracts cavity shortening by increasing the refractive index, but cannot correct for cavity lengthening.

We tested and quantified self-stabilization by modulating the laser repetition rate to act as a controlled vibration. This is equivalent to modulating the OPO cavity length, but easier to control precisely. For small modulation amplitudes, the OPO output intensity tracks changes in the pump repetition rate, as seen from the linear slope in the left peak of Fig. 8. Thermal damping would be expected to be ineffective for fast modulations, and stronger for slow modulations. To check this, while locking the pump CEO to a constant 70 MHz, we frequency-locked the pump repetition rate directly to an RF local oscillator, rather than to the optical reference. The repetition rate then tracked the local oscillator, which was modulated by ± 100 Hz (± 172 nm in oscillator roundtrip cavity length) at five speeds from 0.2 to 5 Hz.

The OPO cavity length was adjusted at the beginning of each measurement to oscillate near the centre of the operating range of the primarily degenerate resonance (intensity ~0.5 in Fig. 8) then left to run freely. Oscilloscope traces of the modulated OPO output are shown on the left of Fig. 9. For fast modulation speeds of 5 and 3 Hz, thermal damping is weak, and the 100 Hz amplitude is enough to sweep through the whole resonance, seen as going from almost no oscillation (zero intensity), through degeneracy (0 to ~0.9 intensity), to nondegeneracy (intensity ~1). Below 1 Hz, the OPO output variation is strongly suppressed. Slower than 0.2 Hz, the artificial modulation becomes comparable to the natural system fluctuations. We find that the amplitude of the modulated OPO output is an offset decaying exponential function of the driving period, with a 1/e time constant of 0.8 s, shown in the right of Fig. 9.

To understand this time constant, we simulated the thermal behaviour of our OPO crystal as a 0.5×2 mm^2 cross-section slab of bulk GaAs with a 2 mm^3 heating volume on one end, and an ideal heat sink 1 cm away on the other end. The simulated crystal had a thermal time constant of 0.64 s, close to our measured value of 0.8 s. To achieve a temperature rise of 8 K in such a model system for slow (~1 Hz) intracavity power variation, absorption in the crystal of ~44 mW is needed. For 2 W of intracavity OPO power, this is a realistic 2% absorption in the OP-GaAs crystal, making thermal effects the likely source of stabilization. Here we note that the 'dynamic' temperature distribution associated with the Gaussian optical beam profile (the OPO beam size at the crystal is ~10 μm) plays a minor role in our case, since the temperature rise in the centre of the beam, as compared to its wings, is too small (0.15 K) and

#246889 Received 30 Jul 2015; revised 9 Sep 2015; accepted 11 Sep 2015; published 1 Oct 2015

the time constant associated with thermal diffusion across the optical beam is too fast (0.4 μs). Thus the main effect in the stabilization process is the heating of the GaAs as a whole.

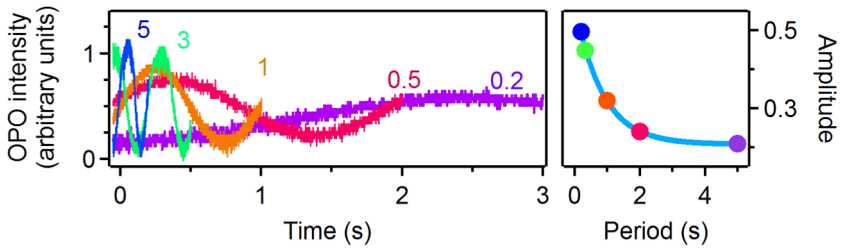

Fig. 9. Left: OPO output as the pump comb repetition rate is modulated by ± 100 Hz at modulation speeds of 0.2, 0.5, 1, 3, and 5 Hz while the OPO is free-running. Right: fit of dependence of modulation amplitude to period, with a 0.8 s exponential time constant, showing that the thermal response of the crystal refractive index counteracts changes on the second timescale.

6. Long term stabilization options

The passive stability of this degenerate OPO is remarkable, but still requires further stabilization for long term use. A simple stabilization method is to use the output power directly as the error signal for side-of-fringe locking. We have used the intensity of the parasite SFG around 1.3 μm to stabilize the OPO cavity length, providing long term stability and low intensity noise. By using the parasite SFG, low-noise near infrared detectors can be used, and part of the midinfrared beam does not need to be diverted. This is similar to the top-of-fringe dithered intensity lock often used for doubly-resonant OPOs [1], but avoids directly dithering the comb line frequencies.

If the goal is simplicity, a stable, monolithic OPO could act as a passive downconversion device, with the pump repetition rate or OPO temperature used for long term corrections. If the goal is superior frequency stability, an existing option is to operate the OPO nondegenerately, and phase lock the OPO to the pump [18, 19], providing frequency stability at the level of the optical reference used, but requiring beat note generation and locking. We have also phase locked the degenerate OPO, by locking the pump CEO against the OPO CEO beat, which acts as an *f*-to-1.5*f* interferometer for measuring half of the pump CEO, and locking the pump to the optical reference as usual. In our case, this leads to a very good lock, as the OPO CEO beat has a signal to noise of about 50 dB at 300 kHz resolution bandwidth on an RF spectrum analyser, and the fast graphene modulator can stabilize the midinfrared output directly. The OPO cavity length can then be used to stabilize intensity and spectral shape. Depending on noise sources, this can reduce intensity or spectral drift by avoiding the coupling of spectral shape and OPO CEO in the nondegenerate case.

7. Conclusions

We have shown that a high-power degenerate OPO can act as a nearly perfect frequency divider for midinfrared frequency comb generation from a stable pump comb, without the need for active stabilization of the OPO. Thermal effects are favourable in this case, providing corrective feedback against cavity length drift.

Our OPO is built with standard laboratory mounts and only conventional room temperature control, so simple engineering improvements could significantly improve passive stability. Higher repetition rates or smaller geometries may improve long term stability by decreasing the OPO size, reducing the effects of thermal expansion. Monolithic degenerate OPOs may one day act as passive downconversion devices for generating narrow linewidth midinfrared frequency combs.

#246889 Received 30 Jul 2015; revised 9 Sep 2015; accepted 11 Sep 2015; published 1 Oct 2015